Revista de Chimie
https://revistadechimie.ro
https://doi.org/10.37358/Rev.Chim.1949

Lead Removal from Aqueous Solutions Using Bean Shells – Equilibrium, Kinetics and Thermodynamic Studies

MILJAN MARKOVIĆ[1*], MILAN GORGIEVSKI[1] (https://orcid.org/0000-0002-9899-719X),
DRAGANA BOŽIĆ[2] (https://orcid.org/0000-0003-1055-8449),
VELIZAR STANKOVIĆ[1] (https://orcid.org/0000-0002-1399-3481),
MILORAD CAKIĆ[3], VESNA GREKULOVIĆ[1],
KRISTINA BOŽINOVIĆ[1] (https://orcid.org/0000-0002-9834-448X)
[1] University of Belgrade, Technical faculty in Bor, Vojske Jugoslavije 12, Bor, Serbia
[2] Mining and Metallurgy Institute Bor, Zeleni bulevar 35, Bor, Serbia
[3] University of Niš, Faculty of Technology in Leskovac, Bulevar oslobođenja 124, Leskovac, Serbia

Abstract: *Lead ions removal from aqueous solutions onto bean shells is presented in this paper. The experiments were conducted in a batch system. The bean shells samples were rinsed with distilled water before the adsorption experiments. The analysis of the rinsed water showed that a significant amount of alkali and alkaline-earth metal ions are transferred from the adsorbent structure into the rinsed solution during the rinsing process. The COD analysis showed that these waters should be treated before being discharged into the surrounding watercourses. The influence of different process parameters (the pH value of the solution, the initial metal ions concentration, and the initial mass of the adsorbent) on the adsorption capacity was investigated. The adsorption capacity was higher at higher pH values of the solution. The adsorption capacity showed a decrease with the increase in the mass of the adsorbent. The increase in the initial metal ions concentration was shown to lead to an increase in the adsorption capacity until 0.8 g dm^{-3}, after which a slight decrease was noted. Characterization of the adsorbent was performed by SEM-EDX, DTA-TGA, and FTIR analysis. The SEM-EDX analysis indicates a change in the morphology of the sample after the adsorption, as well as that K and Mg are possibly exchanged with lead ions during the adsorption process. The results obtained by the DTA-TGA analysis showed a weight loss of 77.8 % in the temperature range from 20°C to 900°C. The FTIR analysis indicated that the amide group is involved in the adsorption process. The pseudo-second order kinetic model was shown to be the best fit for the analyzed data, which led to the conclusion that chemisorption was a possible way of binding lead ions onto the surface of the bean shells. The Hill isotherm model was the best model for the analyzed adsorption equilibrium data. Obtained thermodynamic data indicated that the adsorption process was spontaneous, endothermic, and disordered, in which lead ions are bound to the surface of the bean shells by chemisorption. The maximum achieved adsorption capacity was 46.36 mg g^{-1}.*

Keywords: *adsorption, bean shells, equilibrium, kinetics, lead ions*

1. Introduction

Water pollution is one of the biggest environmental issues today, as a result of an increase in the waste generated by the industrial activities, that are often discharged into the surrounding watercourses without prior treatment [1].

The continuous water pollution by heavy metals leads to an increased research activity focused on how to remove these pollutants from the environment. One of the most researched heavy metal, among others, is lead (Pb) [2].

Industrial wastewaters originate from factories and various industrial plants, as a result of clean water being used in the production process. These waters contain many toxic materials [3]. Inadequate treatment of industrial wastewater can lead to pollution of surrounding streams, rivers, lakes, etc. [4].

**email: mmarkovic@tfbor.bg.ac.rs, (https://orcid.org/0000-0002-4734-1481)*

Heavy metals can be removed from wastewaters by well-known conventional technologies, such as ion exchange, solvent extraction-electrowinning (SX-EW), chemical precipitation, etc. These technologies have many disadvantages, like high cost, continuous input of chemicals, incomplete metal removal, and others. These disadvantages raise the importance of the biosorption as a new method that could become an alternative to the existing conventional technologies for industrial wastewater treatment, with a low content of heavy metal ions [5].

Due to the tendency of every industrial process to be more economically efficient, potential alternative methods of wastewater treatment are investigated. One of the potential alternatives to existing conventional technologies for wastewater treatment, especially those with low heavy metal ions content, is adsorption using natural adsorbents - biosorption. Biosorption is based on the possibility of certain biomolecules or biomass to selectively bind ions or other molecules from aqueous solutions. The main advantage of biosorption versus conventional purification methods, in addition to its efficiency in the removal of metal ions, is the availability and price of such adsorbents, which tend to have small or no economic value [6 - 11].

Lead is dangerous pollutant, toxic for plants, animals, micro-organisms, and humans. It bio-accumulates in most living organisms. In waters, lead can reach human organism through drinking water and through the food chain [12]. Lead is used in the production of batteries, in electrowinning, for printing, production of photographic material, pigments, etc. Wastewaters from these industries usually have a low *p*H value and contain high concentrations of heavy metals, including lead, so it is necessary to treat these waters before discharging into surrounding watercourses [13].

Biological materials that have an affinity for the metal ions that need to be removed can be used as biosorbents in the adsorption process. One of the biggest challenges of the biosorption process itself is the selection of the right biomass [14].

Various waste biomaterials were used in the adsorption process, including kiwi and banana peel [15], onion and garlic peels [16], sawdust of deciduous trees [17], wheat straw [18], beech sawdust [19], and many others.

In the literature not many authors have examined the possibility of the use of bean shells as an adsorbent for the adsorption of heavy metal ions from aqueous solutions. In the work of Zhou, et al., mung bean shells were used to remove methylene blue from aqueous solutions with good results, and a considerable adsorption capacity of 165.92 mg g^{-1} [20]. The work of Okwunodulu and Mgbemena suggests that oil bean seed shell is a good adsorbent for Cu^{2+}, Ni^{2+} and Pb^{2+} ions. The obtained adsorption capacity was 98.782 mg g^{-1} for Cu^{2+} ions, 99.986 mg g^{-1} for Ni^{2+} ions and 99.999 mg g^{-1} for Pb^{2+} ions [21].

The aim of this paper is to characterize the bean shells as an adsorbent, to determine whether they could be used efficiently for lead ions removal from water solutions, as well as to analyze the impact of different parameters on the biosorption process.

The novelty in this paper would be that bean shells as an adsorbent is insufficiently, or almost not at all, examined to remove metal ions from aqueous solutions. In this regard, this paper contributes to a detailed study of the use of bean shells as an adsorbent for the adsorption of lead ions from aqueous solutions. The performed analysis and obtained results indicate that bean shells can be a very effective adsorbent for lead ions adsorption.

2. Materials and methods

2.1. Chemicals

Adsorption experiments were conducted using synthetic Pb^{2+} solutions (0.2 g dm^{-3} initial concentration). Solution were prepared with $Pb(NO_3)_2$.

COD of the rinsate of the bean shells was determined using the 0.005 M $C_2H_5O_4$ and 0.002M $KMnO_4$ solutions.

The effect of *p*H value on the adsorption capacity was determined by adjusting the *p*H values of the solutions with 0.1 M HNO_3 and 0.1 M KOH solutions. The cation exchange capacity CEC was determined using the 1 M NH_4Cl solution. All the chemicals were of p.a. quality.

2.2. Adsorbent

Bean shells, used as an adsorbent for the adsorption experiments, were collected on the fields in a village Rudna Glava, located near the town of Majdanpek (Eastern Serbia). Collected bean shells were ground, and sieved through a set of laboratory sieves. The -1 +0.4 fraction was used for further adsorption experiments.

Figure 1 shows raw bean shells sample.

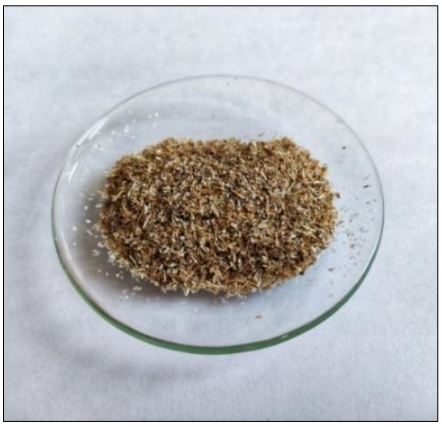

Figure 1. Raw bean shells sample

For the characterization of the bean shells, the following experiments and analysis were performed:

- Characterization of the adsorbent:
- Chemical composition
- Chemical oxygen demand
- Cation exchange capacity
- SEM-EDS analysis
- DTA-TGA analysis
- FTIR analysis
- Point of zero charge

2.3. Characterization of bean shells

The chemical composition of bean shells

The bean shells sample was burned and the ash was used to determine the chemical composition of the sample. Chemical analysis of the obtained ash was performed by ICP-AES and ICP-MS methods on the SPECTRO BLUE and AGILEND 7700 device, respectively.

Determination of COD in the rinsing water

The COD in the rinsing water was determined volumetrically by titrating the rinsing water with a 0.02 M $KMnO_4$ solution. The COD was determined to be 39 mgO_2/dm^3. According to the ecree on limit values of pollutants in surface and groundwater in Serbia (Official Gazette of RS, No. 50/2012) [22], such waters belong to the fourth class of wastewater, which is why they must not be discharged into the surrounding watercourses without prior treatment.

The cation exchange capacity (CEC)

Cation exchange capacity (CEC) is the ability of a material to adsorb cations from water solutions. The CEC between the bean shells and the liquid phase was determined volumetrically, by the ion exchange method, using NH_4Cl solution, during which the ammonium ions from the solution were exchanged with the alkali and alkaline earth metal ions from the structure of the bean shells [23].

SEM-EDS analysis

The morphology of the bean shells before and after Pb^{2+} ions adsorption was examined by a SEM scanning electron microscope (VEGA 3 LMU TESCAN) with integrated energy-dispersive X-ray detector (X-act SDD 10 mm^2, Oxford Instruments). Before the SEM analysis, the samples were steamed with thin layer of chromium in the sputter coater (QUORUM Q150T ES) to become conductive. These samples were then transferred into the microscope chamber and observed at a voltage of 8 kV.

DTA-TGA analysis

The DTA-TGA analysis of a bean shells sample was performed on a simultaneous DSC-TGA device (SDT Q600) under an inert nitrogen atmosphere. 3.5 mg of bean shells sample was heated at a constant rate of 10°C/min at the temperature interval from 20 to 900°C.

FTIR analysis

The infrared spectra of the analyzed samples was recorded by a Bomem MB-100 (Hartmann & Braun, Canada) FTIR spectrometer, in the range of 4000 - 400 cm^{-1}, at resolution of 2 cm^{-1} with 16 scans. The samples were compressed in a potassium bromide (KBr) tablets prior to analysis. Obtained FTIR spectra were then analyzed by Win Bomem Easy software.

2.4. Adsorption experiments procedure

The adsorption experiments were performed in batch conditions, in laboratory beakers equipped with a magnetic stirrer, in order to keep the adsorbent in the suspension. Adsorption conditions, like temperature, *p*H value of the solution, initial lead ions concentration, initial mass of the adsorbent, were modified, depending on the experiment. After conducting the experiments, the suspension was filtered, and the filtrate analyzed for lead ion content. All experiments were carried out at ambient temperature, except for thermodynamic studies.

Adsorption capacity was calculated using the following equation [18]:

$$q(t) = \frac{c_i - c(t)}{m} V \quad (1)$$

where *q(t)*- is the adsorbent capacity defined as mass of the adsorbed metal per unit mass of the adsorbent (mg g^{-1}) at time t; c_i and *c(t)*- are the initial and actual concentrations of metal ions (g dm^{-3}) at time *t*; *V*- is the volume of the solution used in the adsorption experiments (dm^{-3}); and *m*- is the mass of the adsorbent (g) [18].

2.5. Adsorption kinetics

Kinetic models are used to determine the adsorption rate, mechanism of the adsorption process, its speed, and time needed to reach the equilibrium. Pseudo-first order kinetic model, pseudo-second order kinetic model, Elovich kinetic model, and the interparticle diffusion kinetic model were used in this paper to analyze the obtained experimental data, as the models most often used in literature [24-26].

Pseudo-first order kinetic model

Pseudo-first order kinetic model was determined by Lagergren. This model assumes that adsorption is a reversible process [27].

The pseudo-first order model can be expressed as:

$$\frac{dq(t)}{dt} = k_1\left(q_e - q(t)\right) \tag{2}$$

where: *q(t)* - is the adsorbent capacity defined as the mass of the adsorbed metal per unit mass of the adsorbent (mg g^{-1}) at time t; q_e– is the adsorption capacity defined as mass of the adsorbed metal per unit mass of the adsorbent (mg g^{-1}) at equilibrium; and k_1 - is the adsorption rate constant for the pseudo-first order kinetic model (min^{-1}).

By integrating the equation (2), the following equation is obtained:

$$\log(q_e - q(t)) = \log(q_e) - \frac{k_1}{2{,}303}\cdot t \tag{3}$$

Plotting $log(q_e-q(t))$ vs. *t* gives a linear dependence, from which the pseudo-first order kinetic parameters can be determined.

Pseudo-second order kinetic model

This model assumes that on the surface of the adsorbent, adsorption and ion exchange takes place, whereby the adsorbate is bound to the adsorbent surface by chemisorption [28].

A nonlinear form of the pseudo-second order kinetic model can be expressed as [29]:

$$\frac{dq(t)}{dt} = k_2\left(q_e - q(t)\right)^2 \tag{4}$$

where: *q(t)* - is the adsorbent capacity defined as the mass of the adsorbed metal per unit mass of the adsorbent (mg g^{-1}) at time t; q_e- is the adsorption capacity defined as mass of the adsorbed metal per unit mass of the adsorbent (mg g^{-1}) at equilibrium; and k_2- is the adsorption rate constant for the pseudo-second order kinetic model (g mg^{-1} min^{-1}) [29].

Rearranging Eq. (4) to obtain its linear form, provides the following equation [29]:

$$\frac{t}{q(t)} = \frac{1}{k_2 q_e^{\,2}} + \frac{t}{q_e} \tag{5}$$

Plot *t/q(t)* vs. *t* is used to determine the pseudo-second order model kinetic parameters.

Intraparticle diffusion (Webber-Morris) kinetic model

The intraparticle diffusion kinetic model assumes that adsorption does not take place only on the surface of the adsorbent, but also includes diffusion and adsorption inside the adsorbent structure [30].

Linear form of this model is given by [31]:

$$q(t) = k_i t^{1/2} + C_i \tag{6}$$

where: *q(t)* - is the adsorption capacity defined as the mass of the adsorbed metal per unit mass of the adsorbent (mg g^{-1}) at time t; k_i -is the internal particle diffusion rate constant (mg g^{-1} $min^{-0,5}$); and C_i - is a constant that provides insight into the thickness of the boundary layer. If the C_i value is higher, the boundary layer effect is greater, so the effect of surface adsorption in controlling the process speed is greater (mg g^{-1}).

Elovich kinetic model

Elovich kinetic model was primarily used for investigating gas chemisorption on solid adsorbents processes. However, this model was later successfully applied on adsorption of toxic materials from aqueous solutions [32]. It is often given in the following form:

$$\frac{dq(t)}{dt} = \alpha e^{-\beta q(t)} \tag{7}$$

where: α- is the starting adsorption rate (mg g^{-1} min^{-1}); β- is the parameter that expresses the degree of surface coverage and activation energy for chemisorption (g mg^{-1}); and $q(t)$ - is the adsorption capacity defined as the mass of the adsorbed metal per unit mass of the adsorbent (mg g^{-1}) at time t.

Rearranging the equation (7) the following expression is obtained:

$$q(t) = \frac{1}{\beta}\ln(\alpha\beta) + \frac{1}{\beta}\ln t \tag{8}$$

From the graph $q(t) = f(lnt)$ the Elovich kinetic model parameters can be determined.

2.6. Adsorption isotherms

Adsorption isotherms provide insight into the mechanism of adsorption of metal ions on a given adsorbent and can be used to determine the maximum adsorption capacity, i.e. the maximum amount of metal that a given adsorbent can adsorb under certain conditions.

In this paper, the non-linear Langmuir, Freundlich, Temkin, Redlich-Peterson and Hill isotherm models were used to describe the Pb^{2+}adsorption process onto bean shells.

Langmuir isotherm model

This model was primarily developed to describe the gas-solid adsorption onto activated carbon. It also found its application in describing the possibilities of different adsorbents. This empirical model assumes that the adsorption occurs in a monolayer [33].

The Langmuir isotherm can be expressed as [18]:

$$q_e = \frac{q_m K_L C_e}{1 + K_L C_e} \tag{9}$$

where C_e - is the equilibrium concentration of metal ions (mg dm^{-3}), q_e - is the equilibrium adsorption capacity (mg g^{-1}), q_m -is the maximum adsorption capacity (mg g^{-1}), and K_L - is the Langmuir equilibrium constant (dm^3 g^{-1}) [18].

Freundlich isotherm model

This model represents the earliest known relationship that describes the non-ideal and reversible adsorption, which is not limited by the formation of a monolayer. It can be applied to multilayer adsorption with non-uniform distribution of the adsorption heat and affinities towards a heterogeneous surface [33].

This model is represented by the following equation [18]:

$$q_e = K_f C_e^{1/n} \tag{10}$$

where C_e - is the equilibrium concentration of metal ions in the solution (mg dm^{-3}); q_e - is the adsorbent capacity defined as mass of the adsorbed metal per unit mass of the adsorbent (mg g^{-1}) at equilibrium; and K_F -is the Freundlich equilibrium constant ((mg g^{-1}) (dm^3 mg^{-1})$^{1/n}$) [18].

Temkin isotherm model

This model is suitable for analysis of multilayer chemical adsorption based on strong electrostatic interactions between positive and negative charges [34].

This model is represented by the following equation [18]:

$$q_e = B\ln\left(K_T C_e\right) \tag{11}$$

where: $B = RT/b$ - is the Temkin constant, which refers to the adsorption heat (J mol^{-1}); b - is the variation of adsorption energy (J mol^{-1}); R - is the universal gas constant (J mol^{-1} K^{-1}); T- is the temperature (K); K_T - is the Temkin equilibrium constant (dm^3 g^{-1}); q_e- is the adsorption capacity (mg g^{-1}) at equilibrium; and C_e - is the equilibrium concentration of metal ions in the solution (mg dm^{-3}) [18].

Hill isotherm model

This model assumes that adsorption is a cooperative phenomenon, according to which the ability to bind ligands at one site on a macromolecule can affect the appearance of other binding sites at the same macromolecule [35].

Hill isotherm model can be expressed as [35]:

$$q_e = \frac{q_{sH} C_e^{nH}}{K_D + C_e^{nH}} \tag{12}$$

where: C_e -is the equilibrium concentration of metal ions in the solution (mg dm^{-3}); q_e- is the adsorbent capacity (mg g^{-1}) at equilibrium; and K_D, n_H, and q_{sH} are constants [35].

Redlich-Peterson isotherm model

This model represents a hybrid combination of the Langmuir and Freundlich models, by which the three parameters are incorporated into an empirical equation [35].

Redlich-Peterson isotherm model is represented by the following equation [35]:

$$q_e = \frac{K_R C_e}{1 + a_R C_e^g} \tag{13}$$

where: C_e - is the equilibrium concentration of metal ions in the solution (mg dm^{-3}); q_e - is the adsorbent capacity (mg g^{-1}) at equilibrium; K_R - is the Redlich-Peterson constant (L g^{-1}); a_R - is a constant (L mg^{-1})^g; and g - is an exponent with values between 0 and 1 [35].

2.7. Thermodynamics of the adsorption

Changes in activation energy (Ea), entropy (ΔS), enthalpy (ΔH), and Gibbs free energy (ΔG) can be determined by analyzing the change in equilibrium constants with temperature [35, 36].

The thermodynamic parameters were calculated using the following equations [34, 36]:

$$K_d = \frac{q_e}{C_e} \tag{14}$$

$$\Delta G^0 = -RT \ln K_d \quad (15)$$

$$\ln K_d = \left(\frac{\Delta S^0}{R}\right) - \left(\frac{\Delta H^0}{RT}\right) \quad (16)$$

$$\ln K_d = \left(\frac{-E_a}{RT}\right) + \ln A \quad (17)$$

where: K_d -is the equilibrium constant (L g^{-1}); q_e - is the adsorbent capacity at equilibrium (mg g^{-1}); C_e -is the equilibrium concentration of metal ions in solution (mg dm^{-3}); ΔG^0- is the Gibbs free energy (kJ mol^{-1}); R - is the universal gas constant (J mol^{-1} K^{-1}); T - is the temperature (K); ΔS^0- is the entropy change (J mol^{-1} K^{-1}); ΔH^0- is the enthalpy change (kJ mol^{-1}); Ea -is the activation energy (kJ mol^{-1}); and A -is a constant [35, 37].

3. Results and discussions

3.1. Chemical composition of bean shells

After determining the moisture and ash content of bean shells which was 7.83% and 7.24%, respectively, the remaining sample was analyzed for the chemical composition, and the results are given in Table 1.

Table 1. Chemical composition of the bean shells ash sample

Oxides	SiO_2	CaO	K_2O	P_2O_5	Al_2O_3	MgO	Fe_2O_3	SO_3	Na_2O	MnO	Other
Content, %	7.23	14.40	44.2	8.46	0.044	9.32	0.049	3.70	1.76	0.028	10.81

As can be seen from Table 1, the K_2O content was dominant in comparison to other oxides.

3.2. Cation exchange capacity CEC of bean shells

CEC of bean shells was determined by bringing in contact 1 g of bean shells sample with 50 mL of 1 M NH_4Cl solution, and stirring the suspension for 24 h. Obtained results are given in Table 2.

Table 2. The amount of alkali and alkaline earth metal ions exchanged in the reaction with 1 M NH_4Cl

Ion	Na^+	K^+	Ca^{2+}	Mg^{2+}
The amount of exchanged ions (mmol g^{-1} of bean shells	0.03	1.15	0.17	0.22

The total cation exchange capacity was calculated, as a sum of all the cations exchanged in the experiment. From data given in Table 2, the CEC was found to be 1.57 mmol Me^{z+} g^{-1}, where Me^{z+} represented the alkali and alkaline earth metal ions exchanged in the adsorption process. It can also be seen that K^+ was the dominant ion with the highest cation exchange capacity of 1.15 mmol g^{-1}. This suggested that the K^+ ions present in the structure of the bean shells would probably be exchanged with Pb^{2+} ions during the adsorption process.

3.3. SEM-EDS analysis of bean shells

The SEM-EDS analysis of bean shells was carried out before and after the biosorption of Pb^{2+} ions. The SEM micrographs, along with the corresponding EDS spectra, before and after the adsorption are shown in Figure 2. Pores and cavities (honeycomb-like structure) could be spotted on the micrograph of

raw bean shells (Figure 2a), which facilitated the penetration of the aqueous phase into the adsorbent structure, where lead ions were adsorbed at the internal active sites [38, 39].

After the adsorption of Pb^{2+} ions (Figure 2c), quite a different morphology of the surface of bean shells was observed. The absence of cavities and channels was evident, with compact and uniformly ordered lamellar structure. The changes in the morphology of bean shells after the biosorption of lead ions occurred due to the incorporation and binding of lead ions to active sites in the adsorbent structure [40].

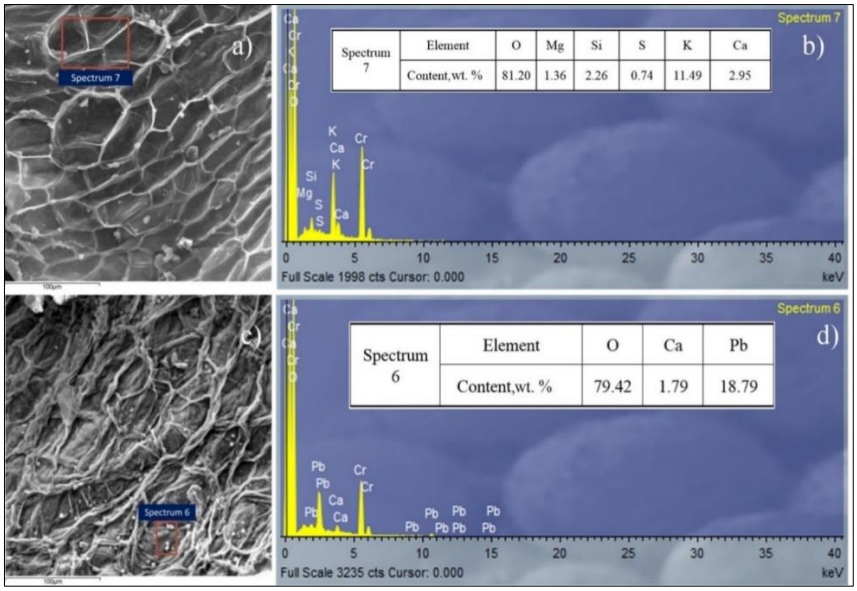

Figure 2. SEM micrograph of bean shells before the adsorption a), and b) the corresponding EDS spectrum with elemental composition analysis of spectrum 7 and after the adsorption c), and d) the corresponding EDS spectrum with elemental composition analysis of spectrum 6

The EDS analysis was performed by recording several points on the surface of the bean shells, before and after the adsorption, to determine the eventual heterogeneous distribution of elements. The EDS analysis was performed in order to determine which chemical elements were present in the sample, as well as to estimate their relative abundance (quantitative analysis). The elements that appeared on the analyzed samples, as well as their content in wt%, are given in Tables attached to Figures 2b and 2d. The EDS results of untreated bean shells (Figure 2b, spectrum 7) showed peaks for O, Mg, Si, S, K, and Ca. The EDS results after the adsorption of lead ions (Figure 2d, spectrum 6) indicated the absence of peaks for K, Mg, Si, and S, while the Ca and O peaks remained but with lower intensity, with new detected peaks for Pb. This was in accordance with the elemental analysis given in Tables (spectrum 6 and 7) attached to Figures 2b and 2d.

3.4. DTA-TGA analysis of bean shells

Thermal analysis provided insight into thermal stability and degradation of a material. The obtained results from the DTA-TGA analysis of bean shells are shown in Figure 3. At TGA curve, a weight loss of 6.68 % in the temperature range from 20°C to 184°C was noticed, as a result of the loss of physically bonded (adsorbed) water within the sample. This process was followed by an endothermic peak on the DTA curve with a minimum at 64.86°C. With further heating, in the temperature range from 184 to 900°C, a weight loss of about 71.12 % was observed on the TGA curve, originating from the degradation of the lignocellulose components present in the bean shells, and the formation of volatile products such as CO, CO_2, and other [41]. In the same temperature range, on DTA curve an exothermic peak was observed, with a maximum at 244.32°C, corresponding to the decomposition of hemicellulose [42]. The total weight loss, in the temperature range from 20°C to 900°C, was 77.8 %.

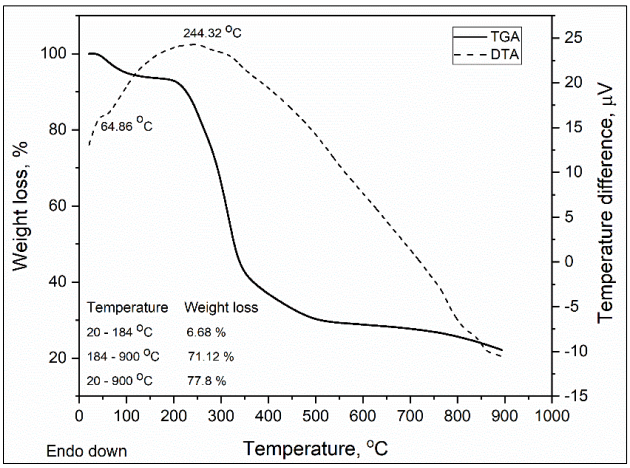

Figure 3. DTA-TGA analysis of bean shells

3.5. Fourier transform infrared spectroscopy (FTIR) analysis of bean shells

The FTIR spectroscopy was performed in order to compare the obtained spectra of before and after the adsorption process, in order to determine which functional groups are responsible for the adsorption of metal ions. Detected adsorption bands in the range from 1300 to 1000 cm^{-1} correspond to -OH, C-OH, and -O-C-O vibrations of the glucoside cellulose groups. Bands in the range from 1000 to 700 cm^{-1} correspond to the deformation of CH groups [43-46].

Bands appearing in the range from 1730 to 1260 cm^{-1} are typical for hemicellulose, and correspond to -C-OH, CH, CH_2 and C=O vibrations. Ones from 1600 cm^{-1} to 1260 cm^{-1} originate from C=C and OCH_3 vibrations, and are typical for lignin. In the low-frequency area, from 600 to 400 cm^{-1}, bands from valent -O-M vibrations are expected, pointing to the metal interactions with the adsorbent [47].

Figure 4 shows the FTIR spectra of bean shells rinsed with distilled water (a), and after the adsorption of Pb^{2+} ions (b). The adsorption bands could be observed on the given spectra, indicating the presence of cellulose, hemicellulose, and lignin. Bands in the range from 1646 to 1530 cm^{-1} (marked with arrows) corresponded to C=O functional groups and deformation of NH vibration (Amide I, and Amide II) of (NH)C=O protein groups, respectively [48].

Comparing these results to the FTIR spectra after the adsorption, it can be recorded that these bands disappeared, and in low-frequency areas, a weak band at around 525 to 480 cm^{-1} appeared, which corresponded to O-Pb valence vibrations [47]. These facts indicated that amide functional groups were involved in the binding of Pb^{2+} ions onto bean shells during the adsorption process.

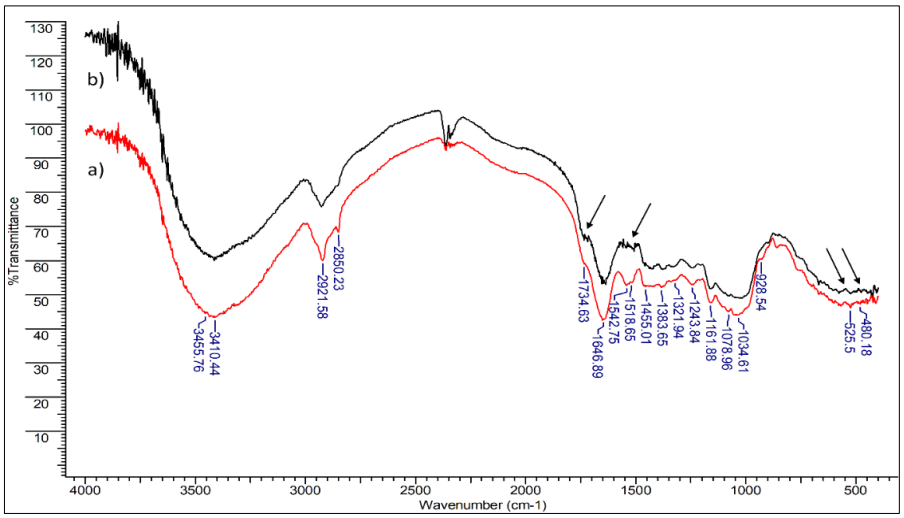

Figure 4. Bean shells FTIR spectrums for samples before (a) and after (b) the Pb^{2+} ions adsorption

3.6. The effect of *p*H value change on the adsorption capacity

To determine the effect of *p*H value on the adsorption capacity, a number of experiments was performed, using a synthetic lead ions solution of different *p*H values, ranging from 2 to 5. The *p*H of the solutions was adjusted with 0.1 M HNO_3 and 0.1 M KOH. The obtained results are presented in Figure 5.

The *p*H of the solution is shown to have a significant effect on the adsorption capacity (Figure 5). As the *p*H of the solution increased, the adsorption capacity increased as well. At *p*H = 2 the adsorption capacity was 11.13 mg g^{-1}, while its maximum value of around 20 mg g^{-1} was achieved at a *p*H = 3. A further increase in the *p*H value did not significantly affect the adsorption capacity.

At low *p*H values, the concentration of H^+ ions is higher, and they occupy active sites in the structure of bean shells, and suppress the already adsorbed lead ions and reduce the adsorption capacity. At higher pH values, active sites on the surface of bean shells could exchange alkali and alkaline earth metals with lead ions from the solution, resulting in a higher adsorption capacity [49].

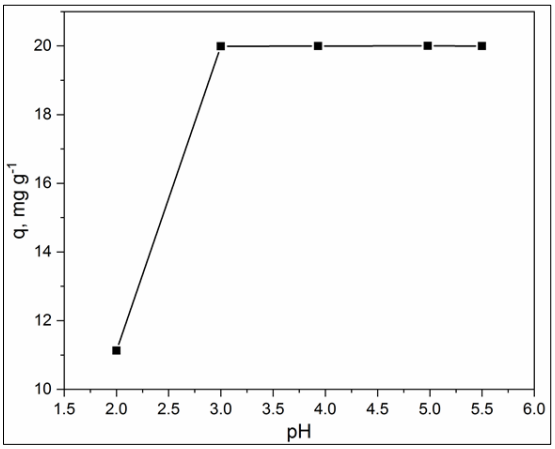

Figure 5. The effect of *p*H value change on the adsorption capacity

3.7. The influence of the change in the mass of the adsorbent on the adsorption capacity and the adsorption degree

The effect of mass change of the adsorbent on the adsorption capacity and the adsorption degree of lead ions onto bean shells was also investigated. The synthetic solution of lead ions with an initial concentration of 0.2 g dm^{-3} was brought into contact with bean shells samples of different initial mass, ranging from 0.1 to 1 g, at a constant stirring rate of 300 min^{-1}. The obtained results are shown in Figure 6.

As can be seen from Figure 6, the adsorption capacity increased with the increase of the initial mass of the adsorbent, due to the increase of specific surface area with an increase of the number of active sites within the structure of the adsorbent [35]. A sharp increase in the adsorption degree was observed with an increase in the mass of the adsorbent from 0.1 to 0.2 g, after which there was no significant change.

However, the adsorption capacity decreased with increasing the mass of the adsorbent. This occurred due to the fact that with the increase of the mass of the adsorbent over 0.2 g, a larger amount of the adsorbent was brought into contact with the solution than it was necessary to adsorb a given amount of lead ions present in the solution [50].

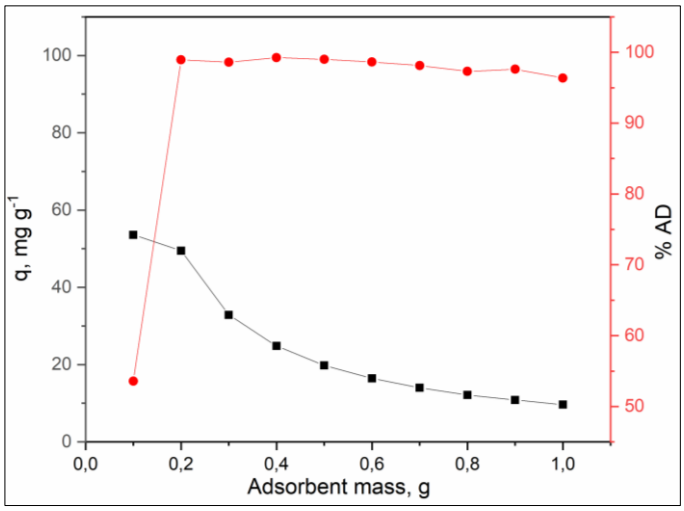

Figure 6. The influence of the change in the mass of the adsorbent on the adsorption capacity and the adsorption degree for lead ions adsorption onto bean shells

3.8. The influence of the initial lead ion concentration on the adsorption capacity

The influence of the initial Pb^{2+} ions concentration on the adsorption capacity was determined by bringing into contact 0.5 g of bean shells with a synthetic solution of lead ions of different concentrations, in the range from 0.002 to 1 g dm^{-3}. The obtained results are shown in Figure 7.

As can be seen from Figure 7, the adsorption capacity increased with the increase of initial concentration of metal ions in solution, reaching a maximum value of 60.12 mg g^{-1} at the initial concentration of 0.8 g dm^{-3} of lead ions, after which it started to decrease. It was assumed that, as the initial concentration of lead ions increased, the probability of their contact with active sites in the adsorbent structure increased, indicating a higher adsorption capacity [51]. With a further increase in the initial concentration of lead ions, after 0.8 g dm^{-3}, a decrease in the adsorption capacity occurred, due to the saturation of the active sites with the lead ions in the molecular structure of the adsorbent.

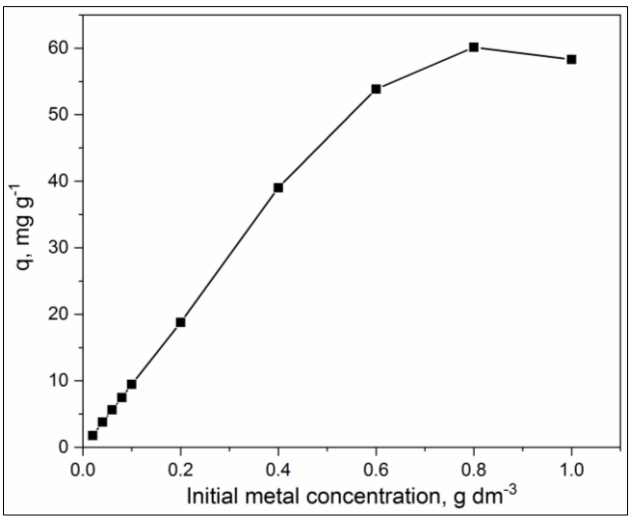

Figure 7. The influence of the initial concentration of lead ions on the adsorption capacity

3.9. Kinetic studies

The change in the adsorption capacity of lead ions with time was determined by a number of experiments, in which the solutions of lead ions with an initial concentration of 0.2 g dm^{-3} were brought into contact with 0.5 g of the sample for different contact time. The adsorption was terminated after 90 min, assuming that this time was long enough to establish the equilibrium in the system [52, 47].

The change in the adsorption capacity of lead ions with time is shown in Figure 8a. It can be seen that at the beginning of the process (5-10 min) the adsorption capacity rapidly increased. It is assumed that this rapid increase in the adsorption capacity was a result of a large number of available active sites in the structure of the adsorbent occupied by lead ions [24].

In this paper, a pseudo-first order kinetic model, a pseudo-second order kinetic model, an intraparticle diffusion kinetic model, and an Elovich kinetic model were used to describe the kinetics of the adsorption of lead ions onto bean shells. Experimental data in Figure 8a were linearized using Eqs. (3, 5, 6, and 8). The corresponding graphs are shown in Figure 8 b-e, allowing the determination of kinetics parameters which are given in Table 3.

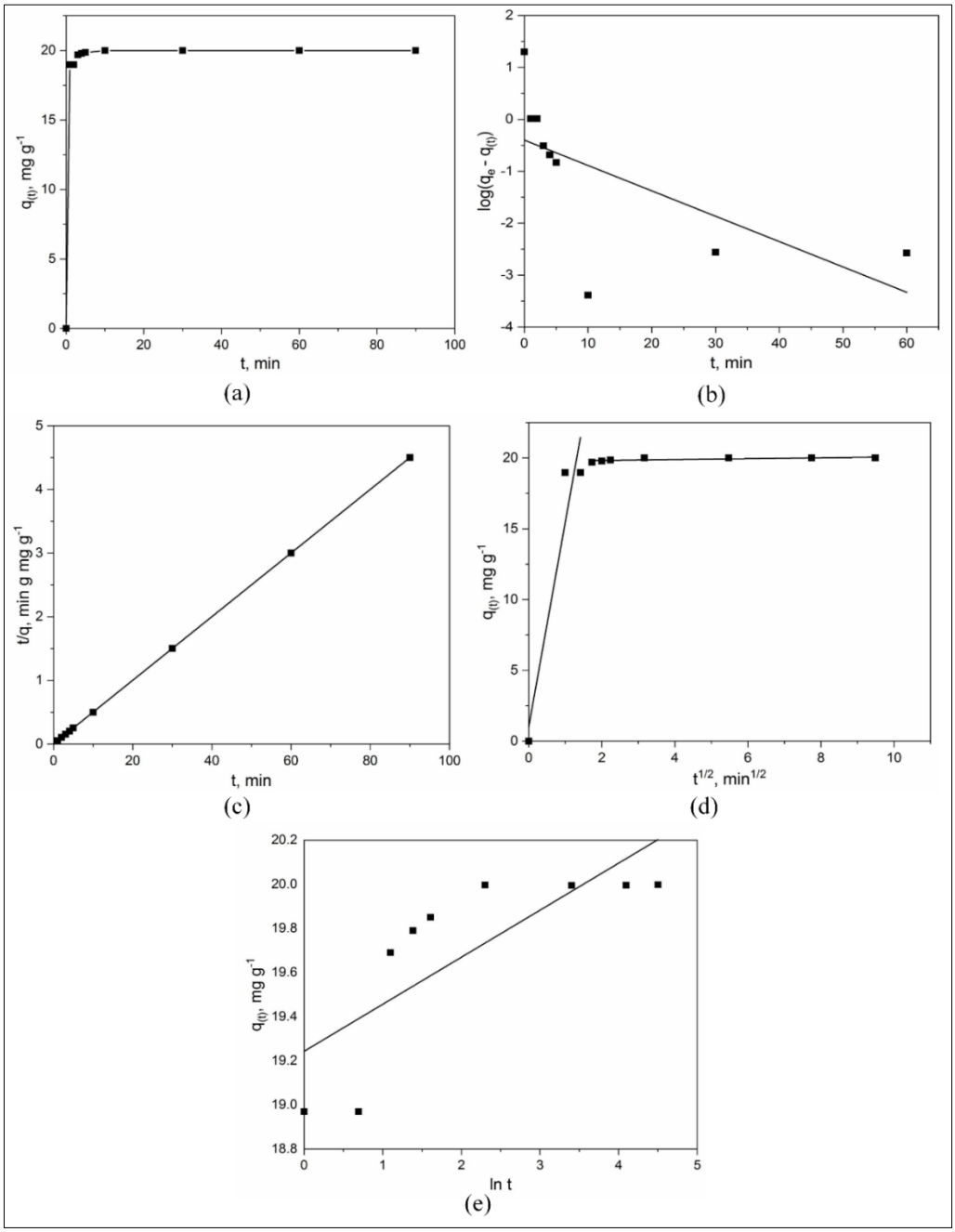

Figure 8. Change in the adsorption capacity with time (a); pseudo-first order kinetic model (b); pseudo-second order kinetic model (c); intraparticle diffusion kinetic model (d); Elovich kinetic model (e)

Table 3. Values of kinetic models constants, adsorption capacity and the correlation coefficient

Model	Parameters	Values
Pseudo-first order kin etic model	k_1 (min^{-1})	0.112
	$q_{e,exp}$ (mg g^{-1})	19.997
	$q_{e,cal}$ (mg g^{-1})	0.397
	R^2	0.415
Pseudo-second order kinetic model	k_2 (g mg^{-1} min^{-1})	1.023
	$q_{e,exp}$ (mg g^{-1})	19.997
	$q_{e,cal}$ (mg g^{-1})	20.012
	R^2	1
Intraparticle diffusion kinetic model	k_{i1} (g mg^{-1} $min^{-0,5}$)	14.44
	C_{i1} (mg g^{-1})	1.026
	R_1^2	0.919
	k_{i2} (g mg^{-1} $min^{-0,5}$)	0.030
	C_{i2} (mg g^{-1})	19.764
	R_2^2	0.545
Elovich kinetic model	α (mg g^{-1} min^{-1})	19.243
	β (g mg^{-1})	0.213
	R^2	0.615

The pseudo-second order kinetic model was determined to be the best fit for the analyzed data (R^2 = 1). The high functionality of the analyzed model was also confirmed by a negligible difference between the values of experimentally determined and calculated adsorption capacity $q_{e,exp}$ and $q_{e,cal}$. Based on this model it can be concluded that the chemical binding of lead ions to the active sites within the structure of the adsorbent was a limiting factor for the adsorption of lead ions onto bean shells [26].

3.15. Isotherm studies

In order to obtain data for the adsorption isotherms the following experiment was performed: 0.5 g of the sample was brought into contact with 50 mL of a synthetic solution of lead ions of different initial concentrations (500 mg dm^{-3}, 300 mg dm^{-3}, 200 mg dm^{-3}, 100 mg dm^{-3}, 50 mg dm^{-3}, 30 mg dm^{-3}, 20 mg dm^{-3}, 10 mg dm^{-3}, and 5 mg dm^{-3}). The suspension was stirred by a magnetic stirrer for 60 min, considering this time long enough to reach the equilibrium between phases [29]. The suspension was then filtered, and the filtrate analyzed on the residual amount of lead ions.

Langmuir, Freundlich, Temkin, Hill, and Redlich-Peterson non-linear isotherm models were used to analyze the experimental data, and the obtained results are shown in Figure 9.

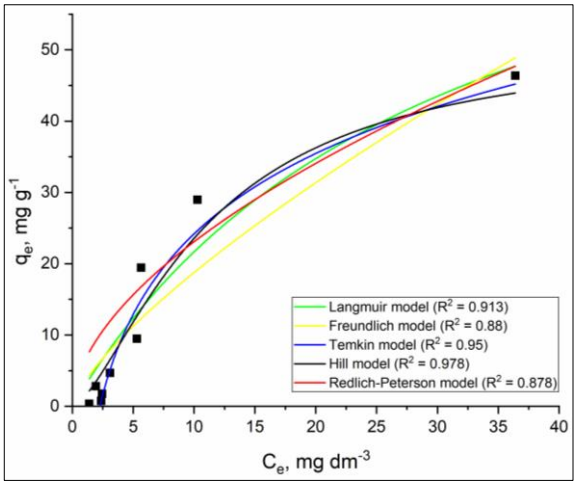

Figure 9. The adsorption isotherm models

The experimental data were fitted using Langmuir, Freundlich, Temkin, Hill, and Redlich-Peterson non-linear isotherm adsorption models, presented in Figure 9, using Eqs. (9) - (13). Observing the correlation coefficients for each model given in Figure 9, it can be concluded that all tested models satisfactorily described the analyzed data, with exception of Hill's model which showed the best

agreement with the experimental data (R^2 = 0.978). According to this model the adsorption of lead ions onto bean shells was a cooperative phenomenon according to which the ability to bind ligands at one site on a macromolecule could affect the appearance of other binding sites on the same macromolecule [33].

3.16. Thermodynamics studies

In order to determine the thermodynamic parameters, 0.5 g of bean shells were brought into contact with 50 mL of a synthetic lead ions solution with a concentration of 200 mg dm^{-3} at three different temperatures (296.9, 303, and 313 K), and stirred for 90 min.

The Gibbs free energy (ΔG^0) was calculated from the experimental data, using equation (15). The enthalpy (ΔH^0), entropy (ΔS^0), and activation energy (Ea) were calculated from the slope and the intercept of the graph ln Kd = f (1/T), respectively [35, 37].

The graph ln K_d = f (1/T) is shown on Figure 10. Based on the experimental data, and the given dependence, thermodynamic parameters were calculated, and the results are given in Table 4.

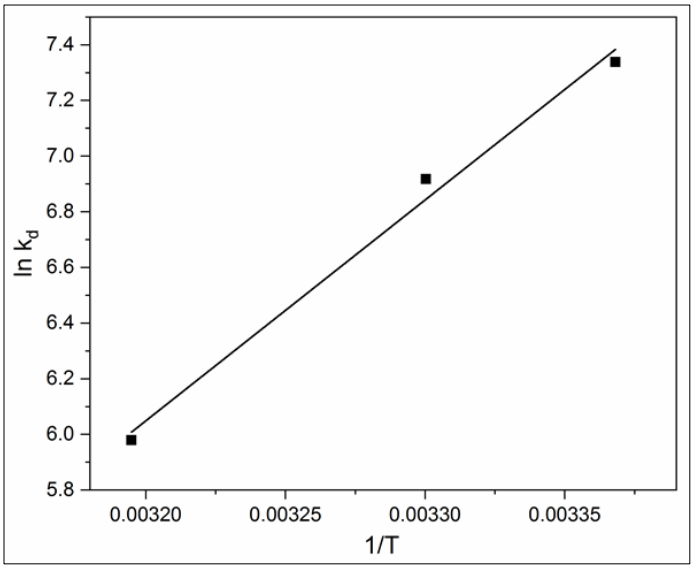

Figure 10. Thermodynamic dependence (ln K_d = f(1/T)) for the adsorption of lead ions onto bean shells

Table 4. Thermodynamic parameters of the adsorption of lead ions onto bean shells

T (K)	ΔG^0 (kJ mol^{-1})	ΔH^0 (kJ mol^{-1})	ΔS^0 (J mol^{-1} K^{-1})	E_a (kJ mol^{-1})
296.9	-18.11	7.9	-19.34	65.986
303	-17.43			
313	-15.56			

It can be seen from Table 4 that ΔG^0 had a negative value at all temperatures, which indicated that the removal of Pb^{2+} ions using bean shells was a spontaneous process.

The enthalpy values lower than 8.4 kJ mol^{-1} indicate that ion exchange is the dominant mechanism of the adsorption of metal ions [52]. The obtained positive value of enthalpy (ΔH^0 = 7.9 kJ mol^{-1}) indicated the existence of an energy barrier and endothermicity of the process [53].

The obtained negative value of entropy (ΔS^0 = -19.34 J mol^{-1} K^{-1}) indicated a decrease in the "disorder" in the liquid-solid intermediate region during the adsorption process. It is assumed that this results were a direct consequence of: (i) changes in adsorbent structure, (ii) increased mobility and depth

of solution penetration within the adsorbent structure, and (iii) predominance of activation energy and enhanced intraparticle diffusion [37].

The activation energy (E_a) of physical adsorption usually does not exceed 4.2 kJ mol^{-1}, while chemical adsorption is based on bonds much stronger than physical ones, and its activation energy is usually in the range of 8.4 to 83.7 kJ mol^{-1}. In this case, the obtained value of activation energy was (E_a = 65.986 kJ mol^{-1}), meaning that the adsorption of lead ions onto bean shells occurred by chemisorption [35].

4. Conclusions

In this work, the characterization of the bean shells biomass was performed, as well as its possible use as an adsorbent for Pb^{2+} ions adsorption analyzed.

After drying and burning the sample, it can be concluded that it contained 7.83 % moisture, 7.24 % ash, and 92.76 organic (combustible) matter.

The COD of the water used to rinse the adsorbent was determined to be 39 $mgO_2\ dm^{-3}$, which leads to the conclusion that these waters must not be discharged into the surrounding watercourses without prior treatment.

The CEC analysis showed a total cation exchange capacity 1.57 mmol $Me^{z+}\ g^{-1}$, with the conclusion that K^+ is the dominant ion in an exchangeable position.

The SEM-EDS analysis, performed before and after the adsorption process, showed that the surface morphology of the bean shells sample changed after the adsorption process, as well as that K and Mg could be exchanged with lead ions during the adsorption process.

The DTA-TGA analysis showed a weight loss of 6.68 % in the temperature range from 20 to 184ºC, as a result of the loss of physically bound water within the sample. Another weight loss of 71.12 % was noticed in the range from 184 to 900ºC, originating from the degradation of the lignocellulose components present in the bean shells sample, and the formation of volatile products, such as CO and CO_2.

The performed FTIR analysis indicated that the amide group is involved in the process of Pb^{2+} ions adsorption onto bean shells.

The point of zero charge (pH_{pzc}) was determined to be 4.32 for the 0.1 M KNO_3 solution and 5.13 for the 0.01 M KNO_3 solution.

The *p*H value of the solution has a significant influence on the adsorption capacity. The adsorption capacity increases with an increase in the *p*H value of the solution, from 10 mg g^{-1} at *p*H 2 to about 20 mg g^{-1} at *p*H values 3 to 5.5.

The adsorption capacity increases with the increase of the concentration of lead ions in the solution until 0.8 g dm^{-3}, where it reaches its maximum value of almost 60 mg g^{-1}, after which it decreases with the further increase of the initial concentration of lead ions.

Kinetic parameters of the Pb^{2+} adsorption process was analyzed using four adsorption kinetic models, the pseudo-first order kinetic model, pseudo-second order kinetic model, Webber-Morris kinetic model, and Elovich kinetic model. The obtained data indicated that the pseudo-second order kinetic model best described the adsorption process, which leads to the conclusion that chemisorption is a possible way of binding lead ions on the surface of bean shells.

The adsorption isotherm data was analyzed using five isotherm models such as: Langmuir model, Freundlich model, Temkin model, Hill model and Redlich-Peterson model. The Hill adsorption isotherm model showed the best agreement with the analyzed data, meaning that the adsorption of lead ions onto bean shells was a cooperative phenomenon, according to which the ability to bind ligands in one place on the macromolecule could affect the appearance of other binding sites at the same macromolecule.

The values of the calculated thermodynamic parameters (ΔG^0; ΔH^0; ΔS^0; and E_a) indicated that the adsorption of lead ions onto bean shells was a spontaneous, endothermic, disordered process, in which lead ions were bound to the surface of the bean shells by chemisorption.

The maximum adsorption capacity was determined to be 46.36 mg g^{-1}.

Acknowledgements: The research presented in this paper was done with the financial support of the Ministry of Education, Science and Technological Development of the Republic of Serbia, within the funding of the scientific research work at the University of Belgrade, Technical Faculty in Bor, according to the contract with registration number 451-03-9/2021-14/ 200131, and the Mining and Metallurgy Institute Bor, Grant No. 451-03-9/2021-14/ 200052. The authors acknowledge our colleagues from the University of Niš, Faculty of Technology in Leskovac, for the FTIR analysis of bean shells samples. Also, the authors want to thank Sandra Vasković, professional English language professor from the University of Belgrade, Technical Faculty in Bor, for the provided language assistance.

References

1. ABBAS, S. H., YOUNIS, Y. M., HUSSAIN, M. K., KAMAR, F. H., NECHIFOR, G., PASCA, B. Utilization of Waste of Enzymes Biomass as Biosorbent for the Removal of Dyes from Aqueous Solution in Batch and Fluidized Bed Column, *Rev. Chim*, **71**(1), 2020, 1-12 https://doi.org/10.37358/RC.20.1.7804
2. MWANDIRA, W., NAKASHIMA, K., KAWASAKI, S., ARABELO, A., BANDA K., NYAMBE I., CHIRWA, M., ITO, M., SATO, T., IGARASHI, T., NAKATA, H., NAKAYAMA, S., ISHIZUKA, M. Biosorption of Pb (II) and Zn (II) from aqueous solution by *Oceanobacillus profundus* isolated from an abandoned mine, *Sci. Rep.*, **10**, 2020, 21189. https://doi.org/10.1038/s41598-020-78187-4
3. VUJEVIĆ, D., MIKIĆ, A., LENČEK, S., DOGANČIĆ, D., ZAVRTNIK, S., PREMUR, V., VINČIĆ, A., Integralni pristup rješavanju problematike industrijskih otpadnih voda, *Inženjersto Okoliša*, **1**, 2014, 25-32.
4. ACHARYA, J., KUMAR, U., RAFI, P. M., Removal of Heavy Metal Ions from Wastewater by Chemically Modified Agricultural Waste Material as Potential Adsorbent - A Review, *Int. J. Curr. Eng. Technol.*, **8,** 2018, 526-530. https://doi.org/10.14741/ijcet/v.8.3.6
5. LONG, M., JIANG, H., LI, X. Biosorption of Cu^{2+}, Pb^{2+}, Cd^{2+} and their mixture from aqueous solutions by *Michelia figo* sawdust, *Sci. Rep.* **11,** 2021, 11527. https://doi.org/10.1038/s41598-021-91052-2
6. STANKOVIĆ, V., BOŽIĆ, D., GORGIEVSKI, M., & Bogdanović G. Heavy metal ions adsorption from mine waters by sawdust, *Chem. Ind. Chem. Eng. Q.* **15,** 2009, 237−249. 10.2298/CICEQ0904237S
7. XUAN, Z., TANG, Y., LI, X., LIU, Y., LUO, F., Study on the equilibrium, kinetics and isotherm of biosorption of lead ions onto pretreated chemically modified orange peel, *Biochem. Eng. J.*, **32**, 2006, 160-164. 10.1016/j.bej.2006.07.001
8. VOLESKY, B., Biosorption and me, *Water Res.*, **41,** 2007, 4017-4029. https://doi.org/10.1016/j.watres.2007.05.062
9. ABDEL-GHANI N.T., EL-CHAGHABY G.A. Biosorption for metal ions removal from aqueous solutions: a review of recent studies, *IJLRST*, **3**, 2014, 24-42.
10. WANG, J., CHEN, C. Biosorption of heavy metals by Saccharomyces cerevisiae – A review, *Biotechnol. Adv.* **24**, 2006 427–451. https://doi.org/10.1016/j.biotechadv.2006.03.001
11. CHEN, X., TIAN, Z., CHENG, H., XU, G., ZHOU, H. Adsorption process and mechanism of heavy metal ions by different components of cells, using yeast (Pichia pastoris) and Cu^{2+} as biosorption models, *RSC Adv.*, **11**, 2021, 17080-17091. 10.1039/D0RA09744F
12.*** World Health Organisation (WHO), 2010.
13. BAJGAI, R. C., JAWED, M., KUMAR, R., Biosorption of Pb ions with rice straw: Kinetics and Characterization study, *BJRD*, **2018**, 14-25.

14. PARK, D., YUN, Y-S., PARK, Y-M., The past, present, and future trends of biosorption, Biotechnol. *Bioprocess Eng.* **15**, 2010, 86-102. https://doi.org/10.1007/s12257-009-0199-4
15. AL-QAHTANI, KHARIA, M., Water purification using different waste fruit cortexes for theremoval of heavy metals, *J. Taibah Univ. Sci.* **10**, 2016, 700–708.
https://doi.org/10.1016/j.jtusci.2015.09.001
16. NAG, S., MONDAL, A., BAR, N., DAS, S. K., Biosorption of chromium (VI) from aqueous solutions and ANN modeling, *Environ. Sci. Pollut. Res.* **24,** 2017, 18817- 18835,
10.1007/s11356-017-9325-6
17. BOŽIĆ, D., STANKOVIĆ, V., GORGIEVSKI, M., BOGDANOVIĆ, G., KOVAČEVIĆ, R., Adsorption of heavy metal ions by sawdust of deciduous trees, *J. Hazard. Mater.* 171, 2009, 684-692. https://doi.org/10.1016/j.jhazmat.2009.06.055
18. GORGIEVSKI, M. (2015). Adsorption of heavy metal ions from aqueous solution using wheat straw as an adsorbent. PhD Thesis, University of Belgrade, Technical faculty in Bor, Serbia.
19. BOŽIĆ, D., GORGIEVSKI, M., STANKOVIĆ, V., ŠTRBAC, N., ŠERBULA, S., PETROVIĆ, N., Adsorption of heavy metal ions by beech sawdust - Kinetics, mechanism and equilibrium of the process, *Ecol. Eng.* **58**, 2013, 202-206. 10.1016/j.ecoleng.2013.06.033
20. ZHOU, H., FENG, Y., WU, Y., YANG, L., Mung Bean Shell (*Vigna radiata* L. Wilczek) - A Novel Cost-effective, Adsorbent for Removing Methylene Blue from Aqueous Solutions, *Adv. Mat. Res.*, **573-574**, 2012, 68-79. http://www.scientific.net/AMR.573-574.68
21. OKWUNODULU, F. U., MGBEMENA N. M., Kinetic studies of oil bean seed shell in the adsorption of toxic heavy metals from their solutions, *Der Chemica Sinica*, **6**, 2015, 52-65.
22.*** Decree on limit values of pollutants in surface and groundwater and sediment and deadlines for their reaching, Official Gazette of RS, No. 50/2012
23. MATIJAŠEVIĆ, S., DAKOVIĆ, A., Adsorption of Uranyl Ion on Acid Modified Zeolitic Mineral Clinoptilolite. *Chem. Ind.* **63**, 2009, 407–414. https://doi.org/10.2298/HEMIND0905407M
24. NAGY, B., MANZATU, C., MAICANEANU, A., INDOLEAN, C., LUCIAN, B. T., MAJDIK, C., Linear and nonlinear regresion analysis for heavy metals removal using *Agaricus bisporus* macrofungus, *Arab. J. Chem.* **10**, 2017, 3569-3579. https://doi.org/10.1016/j.arabjc.2014.03.004
25. WITEK-KROWIAK, A., SZAFRAN, R. G., MODELSKI, S., Biosorption of heavy metals from aqueous solutions onto peanut shell as a low-cost biosorbent, *Desalination*, **265**, 2011, 126-134. https://doi.org/10.1016/j.desal.2010.07.042
26. XIE, S., YANG, J., CHEN, C., ZHANG, X., WANG, Q., ZHANG, C., Study on biosorption kinetics and thermodynamics of uranium by *Citrobacter freudii*, *J. Environ. Radioact.* **99**, 2008, 126-133.
10.1016/j.jenvrad.2007.07.003
27. LAGERGREN, S., About the theory of so-called adsorption of soluble substances, *Sven. Vetenskapsakad. Handingarl*, **241**, 1898, 1-39.
28. COLEMAN, N.T., MCCLUNG, A.C., MOORE, D.P. Formation constants for Cu(II) peat-complexes, *Science* **123**, 1956, 330-331. 10.1126/science.123.3191.330
29. GORGIEVSKI, M., BOŽIĆ, D., STANKOVIĆ, V., ŠTRBAC, N., ŠERBULA, S. Kinetics, equilibrium and mechanism of Cu^{2+}, Ni^{2+} and Zn^{2+} ions biosorption using wheat straw, *Ecol. Eng.* **58**, 2013, 113-122. https://doi.org/10.1016/j.ecoleng.2013.06.025
30. CHEUNG, W. H., SZETO, Y. S., MCKAY, G., Intraparticle diffusion processes during acid dye adsorption onto chitosan, *Bioresour. Technol.* **98**, 2007, 2897-2904. 10.1016/j.biortech.2006.09.045
31. WEBER, W.J., MORRIS, J.C. Kinetics of adsorption on carbon from solution, *J. Sanit. Eng. Div.* **89** (2), 1963, 31–59.
32. QIU, H., LV, L., PAN, B., ZHANG, Q., ZHANG, W., ZHANG, Q. X., Critical review in adsorption kinetic models, *J. Zhejiang Univ. Sci.*, **10**, 2009, 716-124. https://doi.org/10.1631/jzus.A0820524
33. FOO, K. Y., HAMEED, B. H., Insights into the modeling of adsorption isotherm systems, *Chem. Eng. Technol.* **156**, 2010, 2-10. 10.1016/j.cej.2009.09.013

34. KHAN, A., WANG, X., GUL, K., KHUDA, F., ALY, Z., ELSEMAN, A. M., Microwave-assisted spent black tea leaves as cost-effective and powerful green adsorbent for the efficient removal of Eriochrome black T from aqueous solutions, *Egypt. J. Basic Appl. Sci.* **5**, 2018, 171-182. https://doi.org/10.1016/j.ejbas.2018.04.002
35.OZEL, H. U., GEMICI, B. T., OZEL, H. B., BERBERLER, E., Evaluating Forest Waste on Adsorption of Cd(II) from Aqueous Solution: Equilibrium and Thermodynamic Studies, *Pol. J. Environ. Stud.*, **28**, 2019, 1-7. https://doi.org/10.15244/pjoes/97357
36. BYSAL, Z., CINAR, E., BULUT, Y., ALKAN, H., DOGRU, M., Equilibrium and thermodynamic studies on biosorption of Pb(II) onto *Candida albicans* biomass, *J. Hazard. Mater.*, **161**, 2009, 62-67. 10.1016/j.jhazmat.2008.02.122
37.THILAGAN, J., GOPALAKRISHNAN, S., KANNADASAN, T., Thermodynamic study on adsorption of Copper (II) ions in aqueous solution by Chitosan blended with Cellulose & cross linked by Formaldehyde, Chitosan immobilised on Red Soil, Chitosan reinforced by Banana stem fibre, *IJSRET*, **2**, 2013, 28-36.
38. COELHO, G. F., GONCALVES, A. C., TEIXEIRA TARLEY, C. R., CASARIN, J., NACKE, N., FRANCZISKOWSKI, M. A., Removal of metal ions Cd(II), Pb(II) and Cr(III) from water by the cashew nut shell Anarcadium occdentale L., *Ecol. Eng.* **73**, 2014, 514-525. https://doi.org/10.1007/s13201-018-0724-8
39.COELHO, G. F., GONCALVES, A. C., SCHWANTES, D., RODRIGUEZ, E. A., TEIXEIRA TARLEY, C. R., DRAGUNSKI, D., CONRADI JUNIOR, E., Removal of Cd(II), Pb(II), and Cr(II) from water usind modified residues of Anacardium occidentale L., *Appl. Water Sci.* **8**, 2018, 95-116.
40. MICHALAK, I., CHOJNACKA, K., MARYCZ, K., Using ICP-OES and SEM-EDX in biosorption studies, *Microchim. Acta* **172**, 2011, 65-74. https://doi.org/10.1007/s00604-010-0468-0
41.WILLIAMS, P.T., BASLER, S., The pyrolysis of rice husks in a thermogravimetric analyser and static batch reactor, *Fuel*, **72**, 1993, 151–159. https://doi.org/10.1016/0016-2361(93)90391-E
42.BRANKOV, S. (2016). The possibilities for application of energy from agricultural biomass pyrolysis. PhD Thesis, University of Novi Sad, Faculty of Technical Science, Serbia.
43. EL-SAYED, G.O., DESSOUKI, H.A., IBRAHIM, S.S, Biosorption of Ni (II) and Cd (II) ions from aqueous solutions onto rice straw, *Chem. Sci. J.*, Volume 2010: CSJ-9.
44. GLIŠIĆ, S., CAKIĆ, M., NIKOLIĆ, G., DANILOVIĆ, B., Synthesis, characterization and anti-microbial activity of carboxymethyl dextrane stabilized silver nanoparticles, *J. Mol. Struct.*, **1084**, 2015, 345-351. https://doi.org/10.1016/j.molstruc.2014.12.048
45. MARKOVIĆ-NIKOLIĆ, D., BOJIĆ, A., SAVIĆ, S., PETROVIĆ, S., CVETKOVIĆ, D., CAKIĆ, M., NIKOLIĆ, G., Synthesis and physicochemical characterization of anion exchanger based on green modified bottle gourd shell, *J. Spectrosc.*, 2018, 1-16. https://doi.org/10.1155/2018/1856109
46. MARKOVIĆ-NIKOLIĆ, D., BOJIĆ, A., BOJIĆ, D., CAKIĆ, M., CVETKOVIĆ, D., NIKOLIĆ, G., The biosorption potential of modified bottle gourd shell for phosphate: Equilibrium, kinetic and thermodynamic studies. *Chem. Ind. Chem. Eng. Q.*, **24** (4), 2018, 319-332. https://doi.org/10.2298/CICEQ171019006M
47.GILL, R., NADEEM, Q., NADEEM, R., NAZIR, R., NAVAZ, S., Biosorption capacity of vegetable waste biomass for adsorption of lead and chromium, *JBES*, **5** (2), 2014, 306-317.
48.CAKIĆ, M., GLIŠIĆ, S., CVETKOVIĆ, D., CVETINOV, M., STANOJEVIĆ, LJ., DANILOVIĆ, B., CAKIĆ, K., Green Synthesis, Characterization and Antimicrobial Activity of Silver Nanoparticles Produced om Fumaria officinalis L. Plant Extract, *Colloid J.*, **80** (6), 2018, 803-813. 10.1134/S1061933X18070013
49.SCHIEWER, S., VOLESKY, B. Ionic strength and electrostatic effects in biosorption of divalent-metal ions and protons, *Environ. Sci. Technol.*, **31**, 1997, 2478–2485. https://doi.org/10.1021/es960751u

50.WANG, G., ZHANG, S., YAO, P., CHEN, Y., XU, X., LI, T., GONG, G., Removal of Pb(II) from aqueous solutions by *Phytolacca americana* L. biomass as a low cost biosorbent, *Arab. J. Chem.*, **11**, 2018, 99-110. https://doi.org/10.1016/j.arabjc.2015.06.011
51. SU, W., YANG, Y., DAI, H., JIANG, L., Biosorption of Heavy Metal Ions from Aqueous Solution on Chinese Fir Bark Modified by Sodium Hypochlorite, *Bioesources*, **10**, 2015, 6693-7008. DOI: 10.15376/biores.10.4.6993-7008
52. ŠOŠTARIĆ, T. (2016) Heavy metals removal from aqueous solution by biosorbent based on apricot stones waste biomass. PhD Thesis, University of Belgrade, Faculty of Agriculture, Serbia.
53. YAKOUT, S. M., ELSHERIF, E., Batch kinetics, isotherm and thermodynamic studies of adsorption of strontium from aqueous solutions onto low cost rice-straw based carbons, *Carbon - Sci. Tech.*, **1**, 2010, 144-153.

Manuscript received: 25.05.2021